# MAGNETIC FIELD CALCULATIONS AND MEASUREMENTS FOR THE FINAL FOCUS ELEMENTS AND BABAR DETECTOR OF THE SLAC B-FACTORY

E.Antokhin, A.Buzykaev, A.Chupyra, A.Dubrovin, D.Fedorov, S.Ganzhur, G.Kolachev, A.Litvinov, A.Medvedko, V.Mikerov, S.Mikhailov, A.Onuchin, Sh.Singatulin, P. Vobly
Budker Institute of Nuclear Physics, Novosibirsk, Russia

M.Berndt, A.Boyarski, R.Coombes, W.Dunwoodie, S.Ecklund, D.Jensen, L.Keller, J.Krebs, H.Lynch, Z.Wolf, N.Yu.
Stanford Linear Accelerator Center, Stanford, USA

R.Aleksan, Ph.Bourgeois, L.Gosset, P.Graffin, G.London, J-Ph.Mols, J-Ch.Toussaint.
Saclay laboratory, France

*Abstract*

A series of 2D and 3D calculations of magnetic field in the region of final focus quads, in the tracking region, in the DIRC shield, and calculations of the force on the SC coil were performed with the use of MERMAID computer code. The comparison of the magnetic measurement results and those of the calculations is presented.

## 1. FIELD IN THE REGION OF THE FINAL FOCUS QUADS Q2, Q4 AND Q5.

Strong influence of interaction point (IP) region quadrupoles on the beam imposes strict requirements on their harmonic contents. Beam studies have shown that the multipole requirement for the harmonics n=3-15 is better then $10^{-4}$ within the beam stay clear region [1,2].

Besides of the conventional nonlinear harmonics in the quadrupoles resulted from their mechanical imperfection and those specifically associated with the end field effects there is also harmonic contents induced by the axial leakage flux from BaBar. This is basically skew octupole component appearing at the ends of the quads due to the angular variation of the axial flux density on their poles. We developed an accurate criteria linking the value of the axial flux on the face of the quad with the value of integrated skew octupole induced by this flux.

We concentrated chiefly on the Q2 quadrupole [2] since it is most effected by the solenoid fringe field. This water-cooled laminated iron quadrupole must accommodate both the high energy ring (HER) and low energy ring (LER), as seen in Fig.1. In order to minimize the end field non-linearity, all quads have mirror plates. Q2 has a mirror only on the IP side.

The end field effects resulting in the appearance of non-linear skew harmonics, chiefly the skew octupole, have been studied on 3D model of Q2 with the use of MERMAID 2D/3D code [4].

Table 1. Parameters of the IP region quadrupoles.

| Quad | $G_0$ [kGs/cm] | $L_{eff}$ [cm] | $\int G\,dz$ [kGs] | $R_i$ [Gs] |
|---|---|---|---|---|
| Q2 | 1.0 | 65 | 65 | 4.78 |
| Q4 | 0.76 | 150 | 114 | 6.65 |
| Q5 | 0.62 | 153 | 95 | 8.0 |

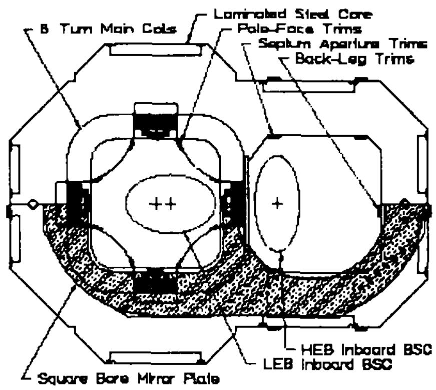


Fig.1 Q2 cross section.

In this model we used a semi-cylindrical problem domain ("iron barrel") with the Q2 located on one side of the "barrel" and a solenoid located on the other side [5]. The solenoid simulates the leakage flux from BaBar. The geometrical parameters of the model, and the current in the solenoid were chosen so that the flux distribution on the face of Q2 is very close to the real. MERMAID 2D/3D allows us to have up to 3 million nodes in the mesh for 256 Mb core memory on Pentium PC. We used just about 1.2 million nodes in the model which was enough to enter the Q2 geometry in all the necessary details and to have an accuracy of the field map high enough to calculate the harmonic contents.

The integral of skew octupole induced by the axial flux on the face of quad may be written [5] as:

$$\int_{z_0}^{\infty} a_4(z)dz = \frac{\alpha}{4}\langle B_z\rangle R_i$$

where $z_0=R_i/4$ is the offset from the pole face, $\alpha$ is the linkage coefficient, $\langle B_z \rangle$ is the average axial field at $z=z_0$ integrated over the same limits, and $R_i$ is the inner bore radius. From the 3D model we obtained the value of linkage coefficient $\alpha$=0.8-0.4 for the end chamfer varying from 0 up to 0.6 $R_i$ respectively. The relative value of skew octupole may be found simply by division of this integral by $G_{eff}R_iL_{eff}$ (see Table 1.). The axial field on the quads may be found numerically from 2D axisymmetrical model or measured directly. Both calculations [5] and measurements were made, and they proved to be in a very good agreement (Fig.2). The most serious situation with the induced skew octupole is at the front of forward Q2 at the IP side where $\langle B_z \rangle$ is up to 120 Gs and therefore the skew terms is order of $3\times10^{-4}$ which is higher than the limitation by a factor 3.

We suggested the method of compensation of the skew octupole induced on the pole face by profiling the mirror plate bore so that the opposite component is induced in the mirror plate. The idea has been numerically modeled on the 3D model of Q2 and then proved by the measurements. The mirror bore was profiled as it shown in Fig.1, it is 96.6 mm square with round corners (box configuration). The mirror plate is 9.5 mm thick and distanced from the core edge by 38 mm. The concentration of the magnetic flux on the poles of the quad creating the octupole is compensated by a decrease of the flux density at the corners of the box bore.

Fig.3 shows the result of the measurements for the box configuration, for the round bore, and without mirror plate.

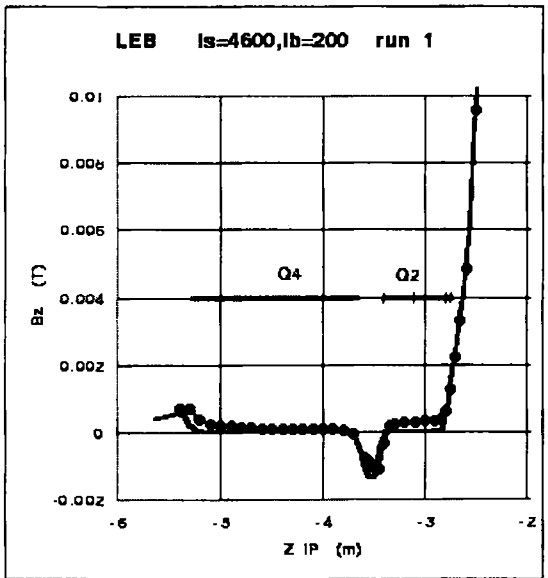


Fig.2 Results of the backward axial field measurements and calculations with the leakage flux compensation.

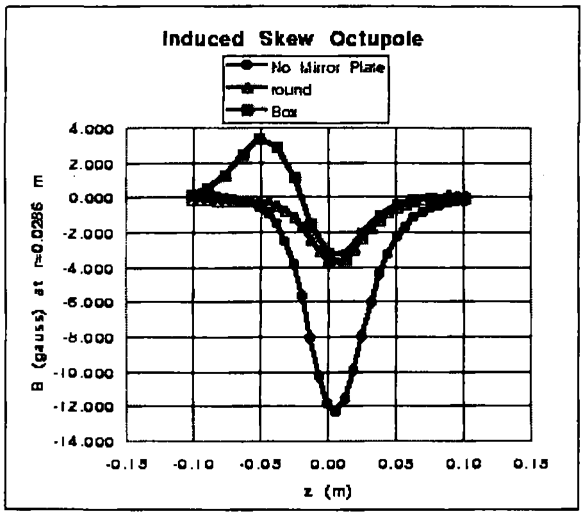


Fig.3 Skew octupole component for the different mirror plate configuration.

The measurements were made with a thin air-core solenoid located at 170 mm from the core edge of a Q2 model, which had the possibility of varying shapes. The field at the core edge was 71 Gs. The integral of the skew octupole is close to 0 for the box configuration. The latter was adopted for the Q2. Annular mirror plates are used at both ends of Q4. The compensation is not required here as the induced skew octupole is far within the requirements.

## 2. FIELD IN THE TRACKING REGION.

The field in the tracking region was measured by a mapper built up at SLAC. There are five 2D and two 1D Hall probes in the mapper. 2D probes were to measure $R$ and $Z$ component of the field while 1D probes measured $\varphi$ component. All probes were calibrated in the test magnet prior the installation. We also used one NMR probe together with the Hall probes. The accuracy of the Hall probes was 0.01%$\times B$+0.6 Gs. The minimal step $\Delta R$ was 7.5 cm.

Figure 4 presents the results of the measurements and calculations of $B_z$ component at $R$=80.5cm which is outer radius of the drift chamber. The agreement is at a level of 10 Gs. Figure 5 shows the variation of $B_r$ with $\varphi$ due to the magnetic axis being tilted with respect to the geometric axis of the steel flux return. A preliminary analysis gives an angle between these two axes of about one mrad.

3D MERMAID calculations of the field in this region also proved to be in a very good agreement with the measurements (Fig.6). The bumps at φ=90° and 270° are easily associated with the vertical chimney cut-out (groove) in the iron poles (doors) triangular in the cross section [3].

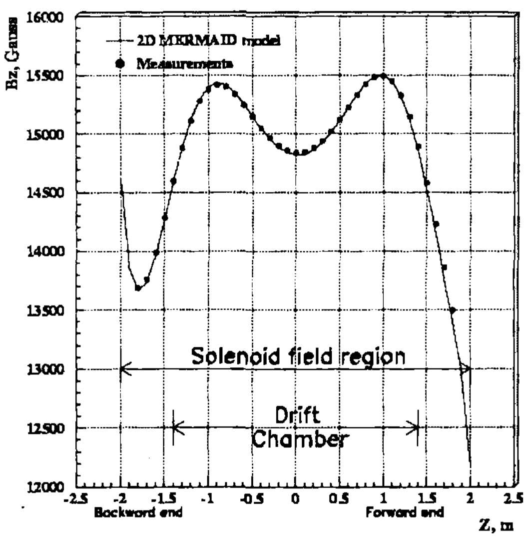


Fig.4 $B_Z(z)$ at $R$=80.5cm.

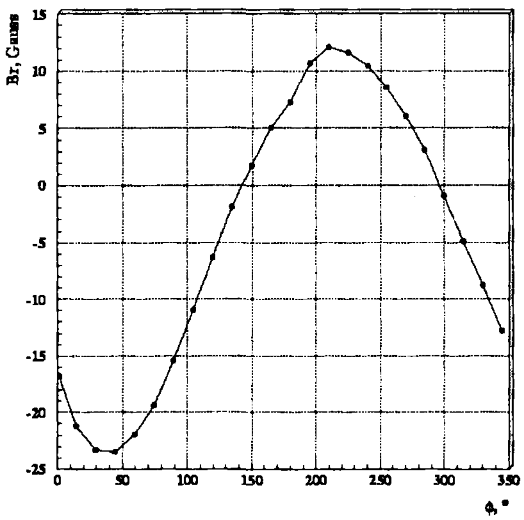


Fig.5 $B_r(\varphi)$ at $Z$=0 and $R$=20.5 cm.

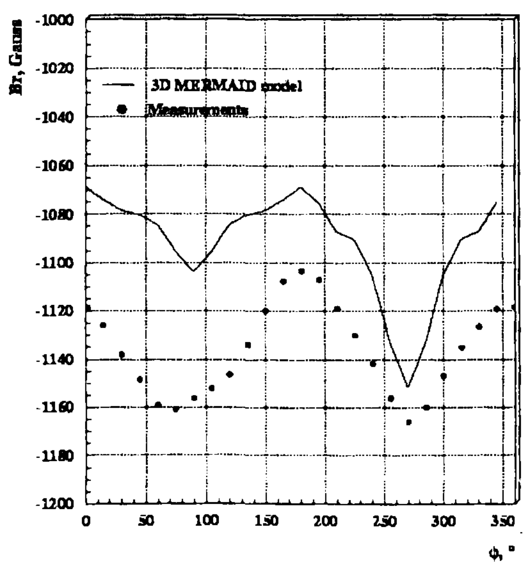


Fig.6 $B_r(\varphi)$ at $Z$=-1.4m and $R$=80.5cm.

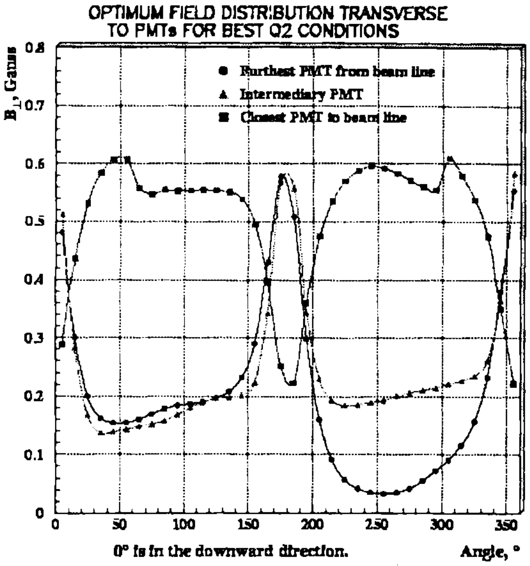


Fig.7 $B_\perp$ component at the PMTs after demagnetization of the DIRC shield.

## 3. FIELD IN THE DIRC SHIELD.

We have calculated and measured the field at the position of the photomultipliers (PMTs) of the DIRC system external to the iron yoke of the detector but within a specially designed iron shield [3]. The measurement system based upon ferro-probes (magnetically modulated permalloy probes) and Hall probes has been designed and fabricated at BINP. The field in the PMT region does not exceed 1 Gs which is in a good agreement with both 2D and 3D calculations [5]. Magnetization of the DIRC shield affecting a great deal the field on the PMTs has been investigated. A simple method of the shield demagnetization reducing the field down to less than 0.6 Gs has been found (Fig.7).

## 4. REFERENCES


[1] "An Asymmetric B Factory Based on PEP: Conceptual Design Report", SLAC-REP-91-372, 1991.

[2] J. Osborn, J. Tanabe, D. Yee, and F. Younger, "Design of the PEP-II Interaction Region Septum Quadrupole, 97 Particle Accelerator Conference, Vancouver B.C., Canada, 12-16 May 1997.

[3] The BaBar collaboration, Technical Design Report, SLAC-REP-95-457, 1995.

[4] Mermaid User's Guide, Novosibirsk, 1994.

[5] E.Antokhin et al., BaBar note 344, SLAC, 1996.